Supporting information for: Conformational dynamics of AcrA govern multidrug efflux pump assembly

Anthony J. Hazel, Narges Abdali, Inga V. Leus, Jerry M. Parks, Jeremy C. Smith, Helen I. Zgurskaya,* and James C. Gumbart*

E-mail: elenaz@ou.edu; gumbart@physics.gatech.edu

Content:

11 pages of supplementary data

Supplementary text

Figures S1 to S3

Tables S1 to S2

References for SI citations

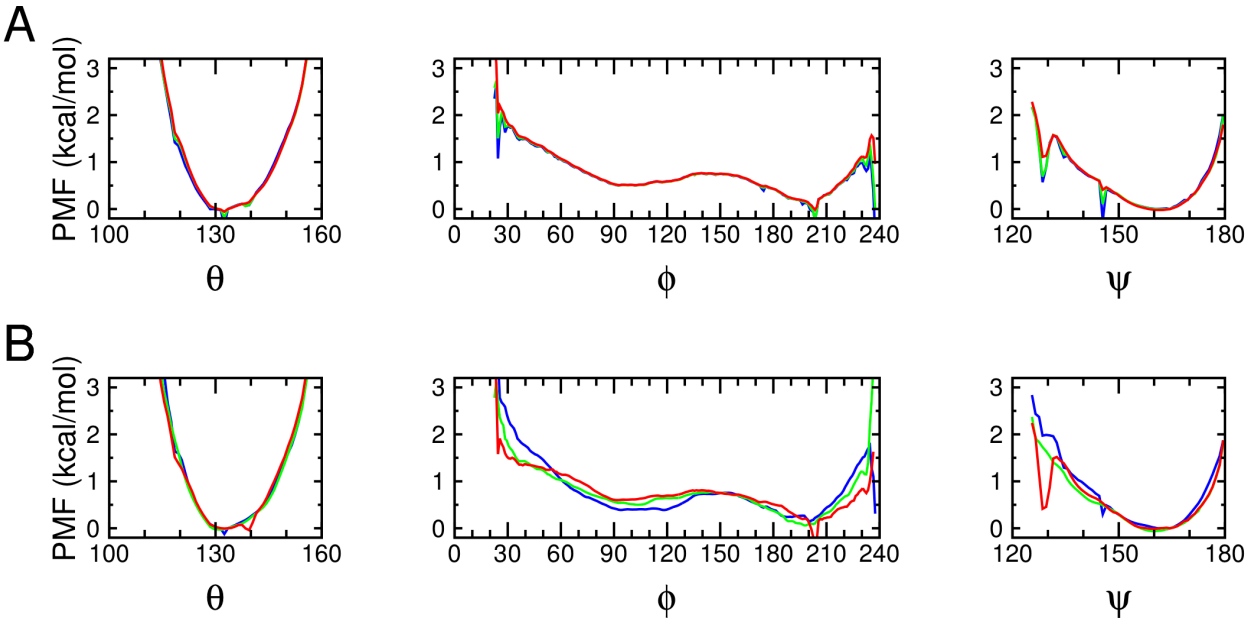

Figure S1: *1D PMFs of free AcrA monomer for each conformational angle.* (A) 1D PMFs calculated from a (blue) unsmoothed, (green) nearest-neighbor averaged, and (red) next-nearest-neighbor averaged 3D PMF. (B) 1D PMFs calculated from (blue) the first 5 ns/window, (green) the second 5 ns/window, and (red) the last 5 ns/window using next-nearest-neighbor averaging.

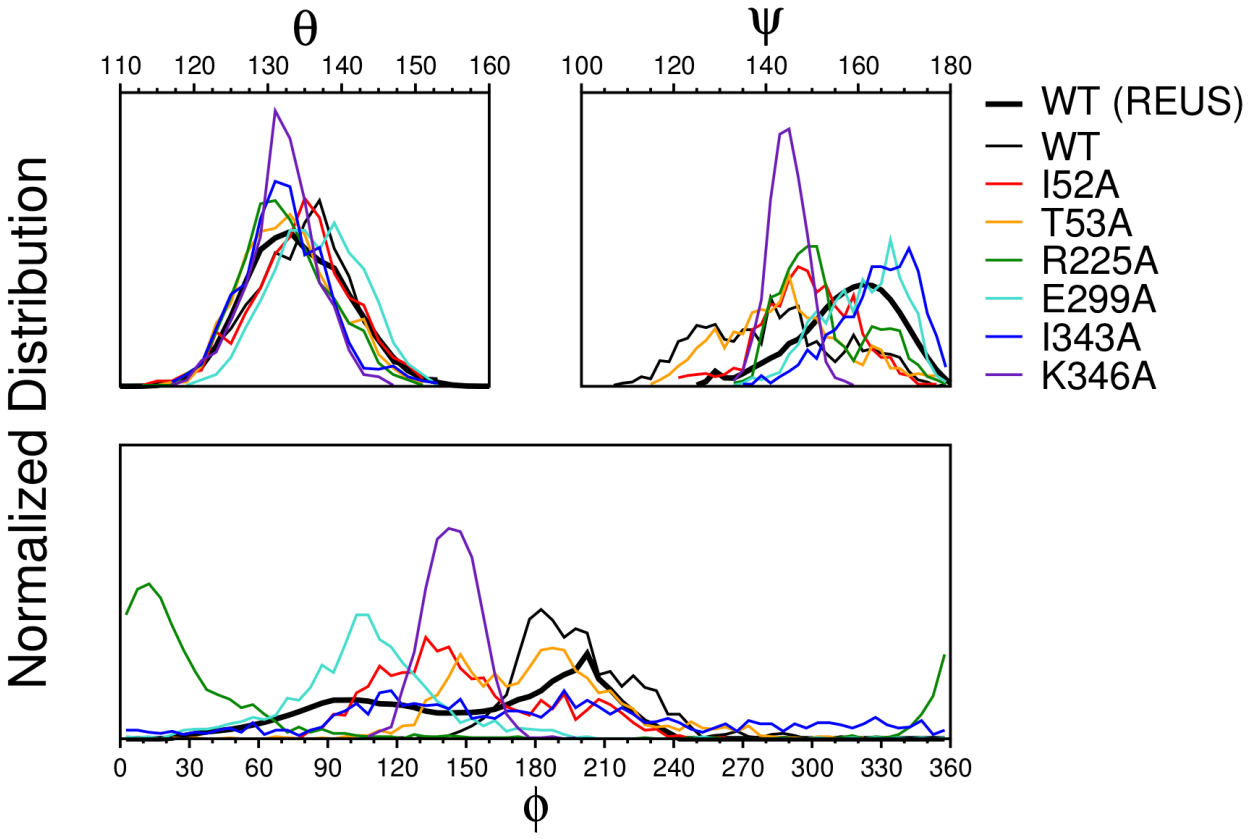

Figure S2: *Distribution of conformational angles from equilibrium simulations.* 250-ns equilibrium simulations of free AcrA monomer in water starting from a bound conformation extracted from Ref.[S1] REUS probability distribution calculated from smoothed 1D PMFs (see Fig. S1, red curve).

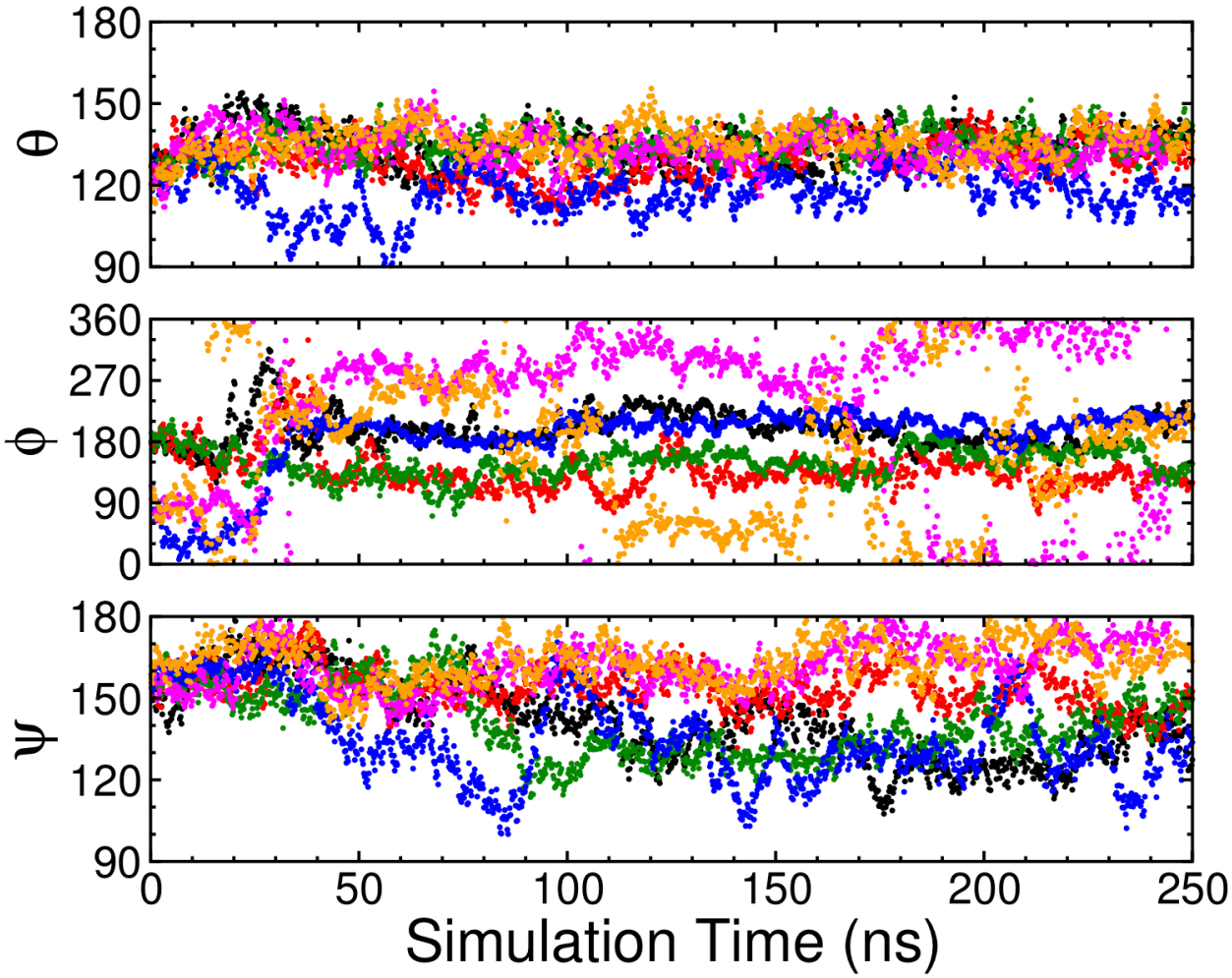

Figure S3: *Trajectories of conformational angles from equilibrium simulations of WT AcrA.* Six 250-ns equilibrium simulations of free AcrA monomer in water starting from bound (black, red, and green points) and unbound (blue, magenta, and orange points) conformations.

Table S1: *Contacts at the interfacial site between the MP and β-barrel domains in the* cis *conformation.* The *cis* conformation is defined as $\phi < 150°$ and $\phi > 240°$. Two residues are considered in contact if their side chains are within 5 Å of each other. Contacts with >30% occupancy in either the REUS or equilibrium simulations, the former reweighted by the free energy, are tabulated below.

Residues		% Occupied	
β-Barrel	MP	REUS	Equilibrium
R225	I343	79.15	35.67
Q228	Q341	66.97	37.68
R225	Q51	50.85	29.17
R225	G344	49.97	7.96
E229	N302	49.96	29.22
E229	Q51	41.55	42.57
Q228	I343	41.14	12.53
N232	Q341	38.59	40.15
L224	I343	37.85	15.59
R225	Q341	37.82	23.14
N221	I343	36.79	17.88
Q228	S340	36.57	28.03
R225	A342	35.15	7.27
N232	S340	34.47	34.02
L224	Q341	33.95	23.46
R225	E299	33.03	0.37
Q228	A342	32.51	3.16
R225	I52	30.99	24.33
E229	I52	6.65	38.23
N232	I343	10.75	32.42
N232	L348	25.12	30.50

Table S2: *Antibiotic susceptibilities of E. coli ΔAcrAB(Pore) cells carrying the plasmid-borne and chromosomally produced AcrAB pump with indicated AcrA variants.*

	No Pore			Pore		
	NOV	ERY	SDS	NOV	ERY	SDS
pUC18	1-2	1	16-32	0.5-1	0.25-0.5	16
WT	**128-256**	**16**	**>1000**	**4-8**	**1-2**	**128-256**
I52A	64-128	16	≥1000	1-4	0.25-0.5	16-32
R225A	128	16	>1000	4-8	2	64
T53A	128	16	>1000	8	2	64
E299A	128	16	>1000	8	2	64
I343A	128	16	>1000	8	2	64
K346A	128	16	>1000	16	2	64-128

Mutations at the interfacial site alter the flexibility of AcrA

Cys-Cys variants of AcrA have revealed how its conformational dynamics govern the stability and function of the AcrAB-TolC efflux pump. To augment these results, we have also examined six single Ala variants – I52A, T53A, R225A, E299A, I343A, and K346A – at the interfacial site between the MP and β-barrel domains using experimental antibiotic susceptibility assays (see Methods in the Main Text) and molecular dynamics (MD) simulations (see Methods below). These data are shown in Table S2 and Figure S3. Most of the Ala variants were able to complement the hypersusceptibility phenotype of ΔAcrAB(Pore)in *E. coli* cells. The I52A variant exhibit a loss of function equivilant to the I52C variant.

We were able to observe some significant changes in the conformational dynamics of free AcrA for these variants (see Fig. S3). Starting from a bound conformation of AcrA extracted from the cryo-EM structure of Jeong et al,[S1] we ran 250-ns of MD simulations for each variant and compared the conformational distributions to the WT variant as well as those from our replica-exchange umbrella sampling (REUS) simulations. Although 250 ns was insufficient simulation time to observe multiple *cis-trans* transitions, we were able to observe some key differences in the conformational dynamics for some of the Ala variants. For example, the I52A and K346A variants exhibited a similar shift in the conformations towards the transition region between the *cis* and *trans* states near $\phi = 150°$, with K346A being much stiffer than I52A. Interestingly, the K346A variant slightly improves function of the pump in the hyperporinated cells, while I52A reduces functionality. The I343A and R225A variants, residues that are both highly involved in inter-domain interactions in the *cis* conformation, also exhibit large, but disparate, changes in conformational distributions. The I343A mutation produces a very flexible AcrA molecule, with almost no energetic barrier between the *cis* and *trans* conformations, while the R225A variant significantly stabilizes the second *cis* conformation near $\phi = 0°$ (see Fig. 3C in the Main Text). Lastly, no significant differences were observed in the T53A and E299A variant distributions when compared against the WT equilibrium and REUS distributions as the two variants remained either in

the *trans* or *cis* distributions, respectively. The severe detrimental affects of the double Cys variants on pump assembly, stability, and function compared to the much less severe and often negligible effects of the single Cys and Ala variants reveal that the flexibility of AcrA, even if the conformational balance is shifted from WT, is a key factor for efficient efflux.

Methods

Equilibrium simulations of free AcrA monomer

For the starting structure of AcrA, we used one of the bound conformations from Ref.[S1] The protein was then solvated with ∼157,000 TIP3P water molecules[S2] in a cubic box of length 168 Å, and then ionized with 0.15 M NaCl, for a total system size of ∼476,000 atoms. The CHARMM36m[S3] force field parameters were used to describe the protein. Hydrogen mass repartitioning[S4] was used for all protein atoms in order to utilize of 4-fs timestep. A 12-Å Lennard-Jones cutoff with switching beginning at 10 Å was used for van der Waals interactions. Simulations were performed using Amber 16[S5] on GPUs. The temperature was held constant at 300 K using a Langevin thermostat. Periodic boundary conditions were used, and the pressure was held constant at 1 atm using the Langevin piston method.[S6] The particle mesh ewald (PME) method was used to describe long-range electrostatics.[S7] Bonds involving hydrogen atoms were constrained to their equilibrium length, employing the SETTLE algorithm[S8] for water molecules and the SHAKE algorithm for all others.[S9] We first ran a pre-equilibration run of 1 ns of WT AcrA, after which AcrA was mutated. Finally, we ran 250-ns production runs of the WT and mutated systems.

References

(S1) Jeong, H.; Kim, J.-S.; Song, S.; Shigematsu, H.; Yokoyama, T.; Hyun, J.; Ha, N.-C. Pseudoatomic structure of the tripartite multidrug efflux pump AcrAB-TolC reveals the intermeshing cogwheel-like interaction between AcrA and TolC. *Structure* **2016**, *24*, 272–276.

(S2) Jorgensen, W. L.; Chandrasekhar, J.; Madura, J. D.; Impey, R. W.; Klein, M. L. Comparison of simple potential functions for simulating liquid water. *J. Chem. Phys.* **1983**, *79*, 926–935.

(S3) Huang, J.; Rauscher, S.; Nawrocki, G.; Ran, T.; Feig, M.; de Groot, B. L.; Grubmüller, H.; MacKerell Jr, A. D. CHARMM36m: an improved force field for folded and intrinsically disordered proteins. *Nat. Methods* **2017**, *14*, 71–73.

(S4) Hopkins, C. W.; Le Grand, S.; Walker, R. C.; Roitberg, A. E. Long-Time-Step Molecular Dynamics through Hydrogen Mass Repartitioning. *J. Chem. Theory Comput.* **2015**, *11*, 1864–1874.

(S5) Case, D.; Betz, R.; Cerutti, D.; Cheatham, III, T.; Darden, T.; Duke, R.; Giese, T.; Gohlke, H.; Goetz, A.; Homeyer, N.; Izadi, S.; Janowski, P.; Kaus, J.; Kovalenko, A.; Lee, T.; LeGrand, S.; Li, P.; Lin, C.; Luchko, T.; Luo, R.; Madej, B.; Mermelstein, D.; Merz, K.; Monard, G.; Nguyen, H.; Nguyen, H.; Omelyan, I.; Onufriev, A.; Roe, D. R.; Roitberg, A.; Sagui, C.; Simmerling, C.; Botello-Smith, W.; Swails, J.; Walker, R.; Wang, J.; Wolf, R.; Wu, X.; Xiao, L.; Kollman, P. *AMBER 2016*; University of California, San Francisco, 2016.

(S6) Feller, S. E.; Zhang, Y. H.; Pastor, R. W.; Brooks, B. R. Constant pressure molecular dynamics simulations — The Langevin piston method. *J. Chem. Phys.* **1995**, *103*, 4613–4621.

(S7) Darden, T. A.; York, D. M.; Pedersen, L. G. Particle mesh Ewald: An N log N method for Ewald sums in large systems. *J. Chem. Phys.* **1993**, *98*, 10089–10092.

(S8) Miyamoto, S.; Kollman, P. A. Settle: An analytical version of the SHAKE and RATTLE algorithm for rigid water models. *J. Comput. Chem.* **1992**, *13*, 952–962.

(S9) Ryckaert, J.-P.; Ciccotti, G.; Berendsen, H. J. C. Numerical Integration of the Cartesian Equations of Motion of a System with Constraints: Molecular Dynamics of n-Alkanes. *J. Comp. Phys.* **1977**, *23*, 327–341.